

Article

# Synthesis and Biophysical Insights into the Binding of a Potent Anti-Proliferative Non-symmetric Bis-isatin Derivative with Bovine Serum Albumin: Spectroscopic and Molecular Docking Approaches

Ali Saber Abdelhameed <sup>1,\*</sup>, Ahmed H. Bakheit <sup>1</sup>, Mostafa S. Mohamed <sup>1</sup>, Wagdy M. Eldehna <sup>2</sup>, Hatem A. Abdel-Aziz <sup>3</sup> and Mohamed I. Attia <sup>1,4,\*</sup>

<sup>1</sup> Department of Pharmaceutical Chemistry, College of Pharmacy, King Saud University, P.O. Box 2457, Riyadh 11451, Saudi Arabia; abujazz76@gmail.com (A.H.B.); mostafanodcar@yahoo.com (M.S.M.)

<sup>2</sup> Department of Pharmaceutical Chemistry, Faculty of Pharmacy, Kafrelsheikh University, Kafrelsheikh 33516, Egypt; wagdy2000@gmail.com

<sup>3</sup> Department of Applied Organic Chemistry, National Research Centre, Dokki, Giza 12622, Egypt; hatem\_741@yahoo.com

<sup>4</sup> Medicinal and Pharmaceutical Chemistry Department, Pharmaceutical and Drug Industries Research Division, National Research Centre, Dokki, Giza 12622, Egypt

\* Correspondence: asaber@ksu.edu.sa (A.S.A.); mattia@ksu.edu.sa (M.I.A.); Tel.: +96-611-467-7337 (M.I.A.)

Academic Editor: Helmut Martin Hügel

Received: 21 May 2017; Accepted: 12 June 2017; Published: 14 June 2017

**Abstract:** As part of the research endeavors to combat cancer, a non-symmetric bis-isatin derivative (compound **3**) was synthesized and showed a significant anti-proliferative potency. The current study provides a comprehensive characterization of the interaction of compound **3** with the drug-transporting protein bovine serum albumin (BSA) via the use of spectroscopic tools along with molecular docking studies. Fluorescence spectral measurements showed that the BSA intrinsic fluorescence can be significantly quenched by the addition of compound **3** and the formation of a non-fluorescent complex. Further measurements revealed a static type of quenching with Stern–Volmer and Linweaver–Burk constants of  $10^5$ . The thermodynamic parameters of the binding were calculated to be  $\Delta S^\circ$   $105.09 \pm 5.32$  with  $\Delta H^\circ$  of  $-0.72 \pm 0.71$  and negative  $\Delta G^\circ$  values. In addition, synchronous fluorescence and 3D fluorescence spectroscopy suggested that compound **3** did not induce conformational changes in BSA. Site competition experiments revealed that compound **3** competes with warfarin within the BSA binding domain (Sudlow site I). This was further confirmed by the molecular docking results showing a binding energy of  $-25.93$  kJ/mol for compound **3**-BSA. Hence, the observed results in the present study assumed that the compound **3**-BSA binding is spontaneous, involving electrostatic forces and hydrogen bonding.

**Keywords:** fluorescence spectroscopy; bovine serum albumin; isatin derivatives; anti-proliferative agent

## 1. Introduction

Cancer is one of the most serious global health problems, constituting the second major cause of death worldwide [1]. The development of new, safe, and effective agents for the management of cancer is still a challenge. Isatin (1*H*-indole-2,3-dione) is an endogenous compound in certain organisms and it was discovered in 1988 [2]. It received considerable attention in the medicinal arena because it is included in a number of bioactive heterocyclic compounds with diverse pharmacological profiles [3–8]. A representative example of an already developed isatin-based anticancer drug is sunitinib (**I**, Sutent<sup>TM</sup>, Pfizer, Inc. New York, NY, USA, Figure 1), which was granted FDA approval in 2006 as an orally active

multi-targeted tyrosine kinase inhibitor used for the management of imatinib-resistant gastrointestinal stromal tumors and metastatic renal-cell carcinoma [9–11]. Semaxanib (II) and orantinib (III) are other examples of isatin-based sunitinib analogs which were developed as new anticancer lead compounds via their multiple tyrosine kinase receptor inhibitory activity (Figure 1) [12].

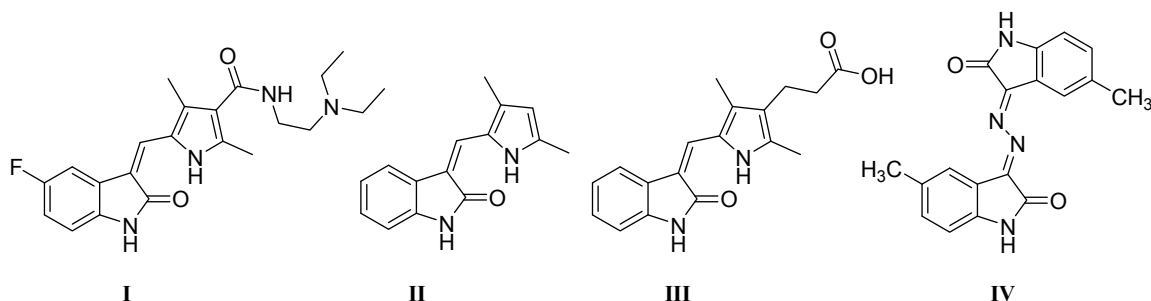


**Figure 1.** Chemical structures of some anticancer agents bearing an isatin nucleus.

It has recently been reported that the symmetric bis-isatin derivative IV exhibited *in vitro* anti-proliferative activity toward the HepG2 cancer cell line with an  $IC_{50}$  value of about 4.23 mM [13]. Accordingly, this represented a strong motif to synthesize the target compound 3 (Figure 2) being a non-symmetric bis-isatin derivative as a new anticancer candidate.

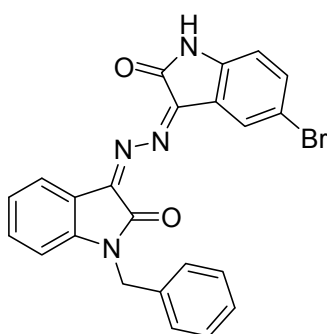


**Figure 2.** Chemical structure of the title compound 3.

Subsequently, and with the advancement of drug development in cancer management along with the synthesis of such potential anti-proliferative agents, numerous probable interactions should be considered. Concurrently, serum albumins, the multi-functional depots and transport carriers, are well known as the principal circulatory proteins in several organisms, forming about 50–60% of the entire number of plasma proteins [14]. Their conformational and physiological characteristics have been comprehensively explored [15–17]. Serum albumins in general are responsible for various conformational dynamics and binding aggregation in solution [18]. The albumin-drug interactions can appreciably control drugs' distribution volume and elimination rate. Hence, drug-albumin investigations may help to interpret a drug's metabolism, transportation mechanism, and its probable pharmacokinetic and pharmacodynamic profiles. A model protein that is frequently used to represent this albumins family in experimental studies is the bovine serum albumin (BSA) [19,20]. BSA is a structural homologue to the human serum albumin (HSA) with a well-studied structure [21–25]. Numerous studies have been published reporting BSA-drug binding interactions using spectroscopic tools [18,20,26,27]. Hence, in the current study, following the successful synthesis of the target non-symmetric bis-isatin derivative, and due to its potential anti-proliferative activity, its interaction with BSA was explored via spectroscopic and molecular docking approaches to gain insight into this compound's molecular features.

## 2. Materials and Methods

### 2.1. Materials

All chemicals, reagents, and solvents were of analytical grade. Bovine serum albumin (BSA) was purchased from Techno Pharmchem (Haryana, India). Ultrapure water used throughout the study was obtained via a Millipore Milli-Q<sup>®</sup> UF-Plus purification system (Millipore, MA, USA).

### 2.2. Chemistry

#### 2.2.1. Synthesis of 5-Bromo-3-hydrazonoindolin-2-one

To a stirred solution of 5-bromoisatin (2.26 g, 10 mmol) in methanol (20 mL), 99% hydrazine hydrate (2.5 mL, 50 mmol) was added. The reaction mixture was refluxed for 1 h. The precipitate was filtered, washed with methanol, and dried to afford 5-bromo-3-hydrazonoindolin-2-one [28] in almost quantitative yield.

#### 2.2.2. Synthesis of 1-benzylindoline-2,3-dione (2)

Benzyl bromide (1.71 g, 10 mmol) was added to a reaction mixture containing isatin (1.47 g, 10 mmol) and potassium carbonate (2.76 g, 20 mmol) in dimethylformamide (15 mL). The reaction mixture was stirred at room temperature for 18 h, poured onto ice-cold water, filtered, and dried to produce 2.18 g (92%) of compound 2 [29], which was pure enough to be used in the subsequent step.

#### 2.2.3. Synthesis of 1-Benzyl-3-((5-bromo-2-oxoindolin-3-ylidene)hydrazono)indolin-2-one (3)

5-Bromo-3-hydrazonoindolin-2-one (0.23 g, 1 mmol) was added to a mixture containing compound 2 (0.24 g, 1 mmol) and included a catalytic amount of glacial acetic acid in ethyl alcohol (10 mL). The reaction mixture was heated to reflux for 6 h, the hot suspension was filtered off, and the collected solid was washed with ethanol. The solid product was re-crystallized from ethanol/DMF mixture (3:1) to yield 0.36 g (79%) of the title compound 3 as a red powder m.p. 265–267 °C; <sup>1</sup>H NMR (DMSO-*d*<sub>6</sub>) *ppm*: 5.01 (s, 2H, CH<sub>2</sub>), 6.89 (d, 1H, Ar-H, *J* = 8.0 Hz), 7.00 (d, 1H, Ar-H, *J* = 8.0 Hz), 7.08 (t, 1H, Ar-H, *J* = 7.5 Hz), 7.27–7.45 (m, 6H, Ar-H), 7.59–7.70 (m, 3H, Ar-H), 11.15 (s, 1H, NH<sub>indolic</sub>); Anal. Calcd. for C<sub>23</sub>H<sub>15</sub>BrN<sub>4</sub>O<sub>2</sub>: C, 60.15; H, 3.29; N, 12.20; Found: C, 59.89; H, 3.33; N, 12.28.

### 2.3. Anti-Proliferative Activity

The anti-proliferative activity of the title compound 3, as well as the reference standard drug, sunitinib, was performed as mentioned in the experimental protocol [30].

### 2.4. Sample Preparation for BSA Binding Studies

Appropriate amounts of compound 3 pure powder were dissolved in dimethyl sulfoxide (DMSO), producing a 2.0 mM solution. A solution of 1 × phosphate buffered saline (PBS buffer) pH 7.4 was used for further dilutions of the compound 3 stock solution to produce a 20.0 μM solution that was used to achieve various working solutions of compound 3. A 15 μM BSA solution was prepared in PBS, and subsequently diluted to a 1.5 μM solution for the measurements. The experimental procedure was performed at ambient temperature and the solutions were then kept at –20 °C.

### 2.5. Instruments and Conditions

Fluorescence spectral determinations were executed on a Jasco FP-8200 (Jasco International Co. Ltd., Tokyo, Japan), with the solutions being measured in a 1 cm quartz cuvette. Values of 5 nm were set for the excitation and emission slit widths, with the emission of the protein monitored at λ<sub>em</sub> = 338 following excitation at λ<sub>ex</sub> = 280. The quenching effect of the ligand on BSA was probed at the emission range (334–344 nm). Emission spectra were recorded in the wavelength range of

290–500 nm. UV-Vis absorbance measurements were accomplished using a Nanodrop™2000 UV-Vis spectrophotometer (Thermo Scientific, Wilmington, DE, USA) with a path length of 1 mm, which is automatically transformed to the absorption results of a conventional 1 cm path length cuvette. Investigational solutions were all prepared in  $1 \times$  phosphate buffered saline (PBS buffer) pH 7.4. Prior to all fluorescence and UV-Vis measurements, blank solutions with the exact used solvents were determined as blank controls and all subsequent measurements were corrected for the solvent's effect. The melting point of the title molecule **3** was measured with Stuart melting point apparatus and was uncorrected. The  $^1\text{H}$  NMR spectrum of compound **3** was run with a 500 MHz Bruker NMR spectrometer (Bruker, Reinstetten, Germany) in deuterated dimethyl sulfoxide ( $\text{DMSO-}d_6$ ). The chemical shift values are expressed in (ppm) using the solvent peak as an internal standard. All coupling constant ( $J$ ) values are given in hertz. The abbreviations used are as follows: s, singlet; d, doublet; t, triplet; m, multiplet. Elemental analysis of the title molecule **3** was carried out at the regional center for microbiology and biotechnology, Al-Azhar University, Cairo, Egypt.

#### 2.6. Protein Concentration Determination

The concentration of the protein was estimated utilizing the specific extinction coefficient of  $\epsilon_{280}^{1\%}$  ~6.7 for BSA using a Nanodrop™ 2000 UV-Vis spectrophotometer (Thermo Scientific, Wilmington, DE, USA).

#### 2.7. Fluorescence Quenching Studies

Spectrofluorimetric investigations of the binding characteristics of compound **3** and BSA were performed at three temperatures (288, 298 and 309 K). Solutions of compound **3** in the concentration range of 0.65–25.0  $\mu\text{M}$  were titrated into a BSA solution of 1.5  $\mu\text{M}$ . The inner filter effect was diminished via the correction of fluorescence intensities arising from excitation and emission light absorption and re-absorption, respectively, utilizing Equation (1) [31,32].

$$F_{\text{cor}} = F_{\text{obs}} \times e^{(A_{\text{ex}} + A_{\text{em}})/2} \quad (1)$$

Where  $F_{\text{cor}}$  and  $F_{\text{obs}}$  are the corrected and measured fluorescence intensities, respectively.  $A_{\text{ex}}$  and  $A_{\text{em}}$  are the compound **3** absorbance readings at excitation and emission, respectively.

#### 2.8. Synchronous and Three Dimensional Fluorescence Measurements

The synchronous fluorescence spectra of the compound **3**-BSA interaction were examined using the wavelength interval ( $\Delta\lambda$ ) values of 15 nm and 60 nm to reveal the tyrosine (Tyr) and tryptophan (Trp) features of the BSA, employing the same concentrations used for the emission determinations. Additionally, three dimensional (3D) fluorescence spectra were determined for a BSA-only solution of 1.5  $\mu\text{M}$  and a mixture solution of BSA and compound **3** (compound **3** concentration of 3.0  $\mu\text{M}$ ) by setting the parameters to an excitation range of 210–350 nm and emission range of 240–610 nm.

#### 2.9. Competitive Binding Using Site Markers

Measurements of the fluorescence intensity of BSA in the presence of compound **3** and warfarin (WAR)/ibuprofen (IBP) as two previously reported site markers for the BSA sites I and II, respectively, were carried out to investigate the binding site for compound **3**. Individual 1.5  $\mu\text{M}$  solutions of BSA and the site markers were made, and compound **3** solutions covering the range of 0 and 25  $\mu\text{M}$  were also prepared.

#### 2.10. UV-Vis Spectrophotometric Determinations

Measurements of the UV-Vis absorption of BSA with and without the addition of compound **3** were accomplished using a range of 220–400 nm. Solutions of 1.5  $\mu\text{M}$  BSA were used with compound **3**

concentrations ranging from 3 to 12  $\mu\text{M}$  for the binding spectral monitoring and 20  $\mu\text{M}$  for compound **3**-only spectral determination.

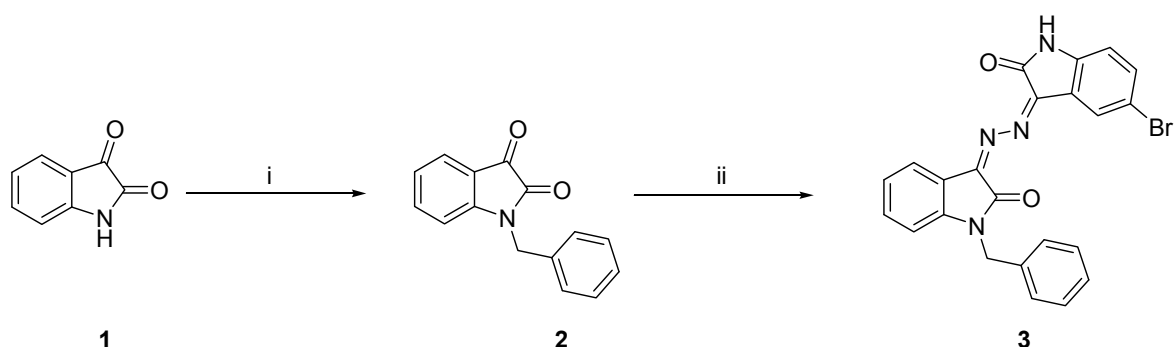
### 2.11. Molecular Docking Studies

The tridimensional crystal structure of BSA was imported from the Protein Data Bank (PDB code 4OR0) [33] into the Molecular Operating Environment software package (MOE<sup>®</sup> 2014; Chemical Computing Group, Montreal, QC, Canada) for a prior optimization that involved the deletion of water molecules and hetero atoms and the supplementation of hydrogen atoms. The compound **3** three dimensional structure was sketched by ChemDraw<sup>®</sup> Ultra 14.0, and the minimized energy structure and geometries of compound **3** were attained by MOE<sup>®</sup> 2014 software. The BSA binding pocket identified, scoring with London dG function, and rescoring with GBVI/WSA dG in MOE<sup>®</sup> were employed to grade the docked poses of compound **3**. The compound **3** configuration with the best score and Root-Mean-Square Deviation (RMSD) values, when bound to BSA, was selected.

## 3. Results and Discussion

### 3.1. Synthesis of the Title Compound **3**

The title compound **3** was prepared as portrayed in Scheme 1. Thus, the commercially available 1*H*-indole-2,3-dione (**1**) was allowed to react with benzyl bromide to furnish the corresponding *N*-benzylated derivative **2**. Subsequently, compound **2** was reacted with 5-bromo-3-hydrazoneindolin-2-one to give the title compound **3**.



**Scheme 1.** Synthesis of the target compound **3**. *Reagents and conditions:* (i) Benzyl bromide,  $\text{K}_2\text{CO}_3$ , DMF, RT, 18 h; (ii) 5-Bromo-3-hydrazoneindolin-2-one, catalytic amount of glacial acetic acid, ethanol, reflux, 6 h.

### 3.2. Anti-Proliferative Activity

Compound **3** showed a potent anti-proliferative activity against human lung (A-549), colon (HT-29), and breast (ZR-75) cancer cell lines as compared with the reference standard anticancer isatin-based drug, sunitinib [30].

### 3.3. Fluorescence Spectroscopic Investigation of the Binding Mechanism

Serum albumins often enhance the apparent solubility of hydrophobic drugs in plasma and modulate their delivery to the cells in vivo and in vitro. The pharmacokinetic characteristics, stability, and toxicity of drugs can be significantly altered as a result of their binding to serum albumins. Bovine serum albumin (BSA) and human serum albumin (HSA) are the major components in plasma protein for cows and humans, respectively. BSA is homologous to HSA, displaying about 88% sequence homology, and consists of three linearly arranged domains (I–III) that are composed of two subdomains (A and B). The use of HSA may be favored over BSA for the studies carried out on clinically used drugs. However, in the present study, for such a compound in the early stages of development, BSA

was employed as a model representing the serum albumins family. Several earlier studies have utilized spectroscopic techniques, particularly fluorescence spectral determination, to explore the different aspects of protein binding to various ligands [34–36]. Fluorescence quenching shows decline protein intrinsic fluorescence occurring through diverse molecular interactions [37,38]. The BSA fluorescence emission spectra with and without the addition of compound 3 were monitored in the wavelength range 290–500 nm upon excitation at 280 nm. The addition of compound 3 caused the BSA fluorescence intensity to be quenched in a concentration dependent way (Figure 3), with no BSA peak shift or shape alteration. The experimental quenching effect can be either classified as a dynamic or a static type of quenching [22,39].

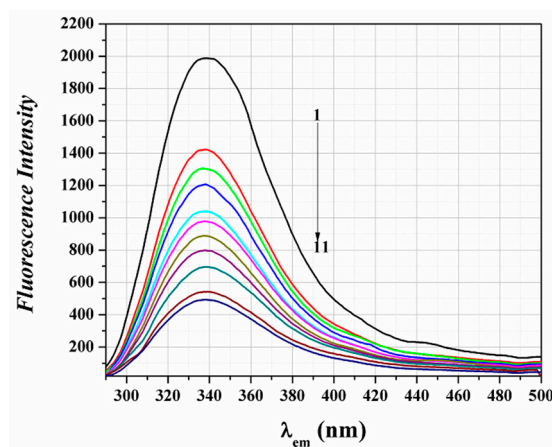


**Figure 3.** Emission spectra of (1) BSA (1.5  $\mu\text{M}$ ) and the BSA-compound 3 system succeeding the addition of compound 3 at the concentrations of (2) 0.65  $\mu\text{M}$ ; (3) 1.0  $\mu\text{M}$ ; (4) 1.5  $\mu\text{M}$ ; (5) 3.0  $\mu\text{M}$ ; (6) 4.5  $\mu\text{M}$ ; (7) 6.0  $\mu\text{M}$ ; (8) 9.0  $\mu\text{M}$ ; (9) 12.0  $\mu\text{M}$ ; (10) 18  $\mu\text{M}$ ; (11) 25  $\mu\text{M}$ .

Based on their temperature dependence, the two types of quenching can be further identified, i.e., higher temperatures yield higher quenching constants in dynamic quenching, while the opposite is always true in the case of static quenching. Hence, the quenching results at the three investigated temperatures were analyzed using the Stern–Volmer (Equation (2)) [40] and Lineweaver–Burk equations (Equation (3)) [41].

$$\frac{F_0}{F} = 1 + K_{SV}C_Q = 1 + K_q\tau_0[Q] \quad (2)$$

$$(F_0 - F)^{-1} = F_0^{-1} + K_{LB}^{-1}F_0^{-1}[Q]^{-1} \quad (3)$$

In the two Equations,  $F_0$  and  $F$  represent the BSA fluorescence intensity alone and when bound to compound 3, respectively, and  $[Q]$  stands for the concentration of compound 3. The Stern–Volmer and Lineweaver–Burk constants are symbolized by  $K_{SV}$  and  $K_{LB}$ , respectively, with  $K_q$  representing the quenching rate constant, and  $\tau_0$  is the mean protein lifetime without compound 3 (quencher) that equals  $(2.7 \times 10^{-9} \text{ s}^{-1})$  [42]. Figure 4a,b show that the compound 3-BSA binding system yields linear Stern–Volmer and Lineweaver–Burk relations with their constants summarized in Table 1. They decline with the gradual temperature rise that then fits well with a static quenching proposal [43]. Furthermore, Equation (4) was employed to estimate the  $K_q$  values listed in Table 1, which are shown to be higher than the formerly reported values for numerous quenchers with the biopolymer of  $2 \times 10^{10} \text{ LM}^{-1} \cdot \text{s}^{-1}$  [42]. Hence, the observed results propose the formation of a complex between compound 3 and BSA [44,45].

$$K_q = K_{SV}/\tau_0 \quad (4)$$

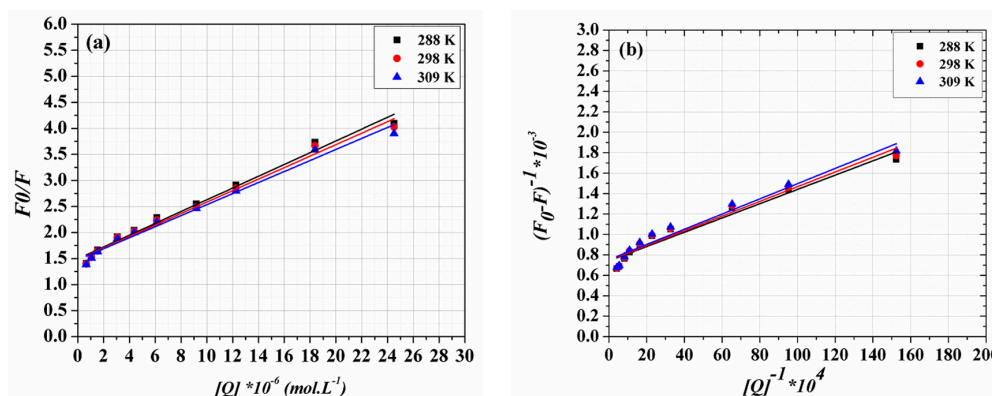


Figure 4. Stern–Volmer (a) and Lineweaver–Burk (b) plots at various temperatures.

Table 1. Parameters computed from both Stern–Volmer and Lineweaver–Burk relations for compound 3-BSA binding.

Temperature (T) (K)	Stern–Volmer Parameters			Lineweaver–Burk Parameters	
	$K_{SV} \times 10^5$ (L·mol <sup>-1</sup> )	$K_q \times 10^{13}$ (L·mol <sup>-1</sup> ·s <sup>-1</sup> )	$r^2$	$K_{LB} \times 10^5$ (L·mol <sup>-1</sup> )	$r^2$
288	1.13 ± 0.047	4.19	0.9863	1.06 ± 0.16	0.9786
298	1.10 ± 0.045	4.08	0.9876	1.04 ± 0.12	0.9798
309	1.06 ± 0.048	3.92	0.9841	1.01 ± 0.12	0.9813

### 3.4. Binding Constant and Number of Binding Sites

Further elaboration of the equilibrium amid the free and bound molecules can be achieved through the analysis of the fluorescence emission data utilizing Equation (5) if we hypothesize the binding of free molecules of compound 3 to equivalent sites on the BSA [43,46]:

$$\log\left(\frac{F_0 - F}{F}\right) = \log K + n \log [Q] \tag{5}$$

Herein,  $K$  denotes the binding constant and  $n$  refers to the number of binding sites on the protein molecule. Hence, plotting the relation between  $\log (F_0 - F)/F$  and  $\log [Q]$  (Figure 5), can yield both  $K$  and  $n$  values. Table 2 summarizes the computed  $K$  and  $n$  values for the compound 3-BSA system at the three experimental temperatures which, consistently with the previous results, shows a decline in the binding constant with the temperature elevation as a result of forming a less stable complex between compound 3 and BSA.

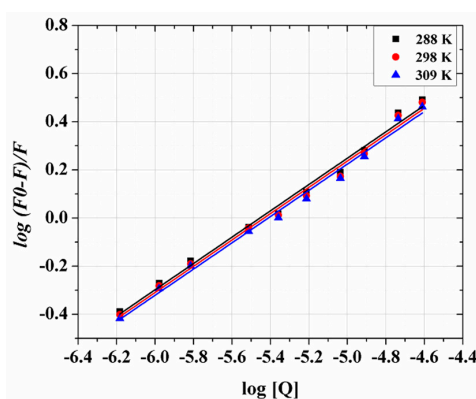


Figure 5. Plots of  $\log [(F_0 - F)/F]$  vs.  $\log [Q]$  for the compound 3-BSA interaction at different temperatures.

### 3.5. Thermodynamics Parameters and Nature of the Binding Forces

Entropy ( $\Delta S^\circ$ ) and enthalpy ( $\Delta H^\circ$ ), as the principal thermodynamic parameters involved in the interaction of compound **3** and BSA, are of significant importance as binding force determinants. Their importance arises from the fact that in such an interaction, the complex formation and the binding constant are highly temperature dependent. In principal, ligand-macromolecule binding can be a result of the involvement of one or more forces, including those that are hydrophobic, van der Waals forces, hydrogen bonding, and electrostatic forces. Former reports have recognized the various forces in protein/ligand binding, in line with the determined thermodynamic parameters [47–49]. Such measurements reveal three potential pathways through which a hydrophobic interaction is claimed if +ve entropy ( $\Delta S^\circ$ ) and enthalpy ( $\Delta H^\circ$ ) values, and hydrogen bonding and/or van der Waals forces could be the driving forces when –ve  $\Delta H^\circ$  and  $\Delta S^\circ$  are observed. Additionally, electrostatic forces are deemed responsible when negative enthalpy ( $\Delta H^\circ$ ) and positive entropy ( $\Delta S^\circ$ ) are present. In the present study, the thermodynamic parameters of the compound **3**-BSA system were computed using Equations (6) and (7):

$$\ln K = \frac{-\Delta H^\circ}{RT} + \frac{\Delta S^\circ}{R} \quad (6)$$

$$\Delta G^\circ = \Delta H^\circ - T \cdot \Delta S^\circ \quad (7)$$

where  $K$  is the association constant and  $\Delta G^\circ$  represents the free energy change. The gas constant and temperature in Kelvins are symbolized by  $R$  and  $T$ , respectively. Accordingly, a plot of  $\ln K$  values against the reciprocal of the temperature (Figure 6) shall be used to compute the values of  $\Delta G^\circ$ ,  $\Delta S^\circ$ , and  $\Delta H^\circ$ .

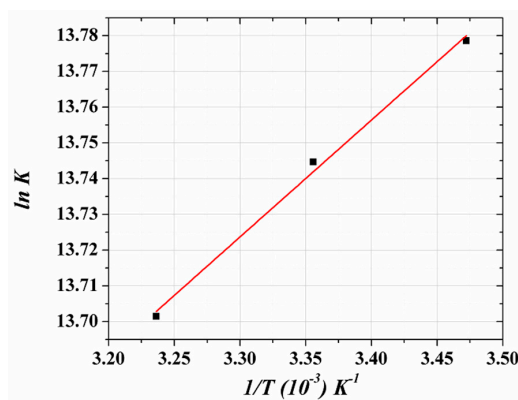


Figure 6. An exothermic Van't Hoff plot for compound **3**-BSA binding.

Based on the previously mentioned rules for the main binding forces, the results summarized in Table 2 revealed that compound **3**-BSA binding cannot be accounted for as a single intermolecular force model. Such values (Table 2) indicate a spontaneous interaction between compound **3** and BSA taking place via hydrogen bonding and electrostatic interactions.

Table 2. Summary of the thermodynamic parameters for the compound **3**-BSA interaction along with binding parameters  $K$  and  $n$ .

Temperature (T) (K)	$\Delta G^\circ$ (kJ·mol <sup>-1</sup> )	$\Delta H^\circ$ (kJ·mol <sup>-1</sup> )	$\Delta S^\circ$ (J·mol <sup>-1</sup> ·K <sup>-1</sup> )	$K \times 10^5$ (L·mol <sup>-1</sup> )	$n^*$	$r^2$
288	$-32.98 \pm 2.5$			$9.65 \pm 0.95$	$0.947 \pm 0.018$	0.9955
298	$-34.04 \pm 2.2$	$-0.72 \pm 0.71$	$105.09 \pm 5.32$	$9.32 \pm 1.20$	$0.946 \pm 0.019$	0.9952
309	$-35.19 \pm 2.3$			$8.92 \pm 0.97$	$0.945 \pm 0.018$	0.9956

\* All values are the average of three determinations.

### 3.6. UV-Vis Absorption Spectra

Figure 7 shows the measured absorption spectra for compound 3 and BSA and proves the formation of a complex between compound 3 and BSA. Moreover, the UV absorption intensity enhanced gradually for BSA following the addition of compound 3 concentrations, which may infer the extension of the BSA peptide strands with the gradual increment of compound 3.

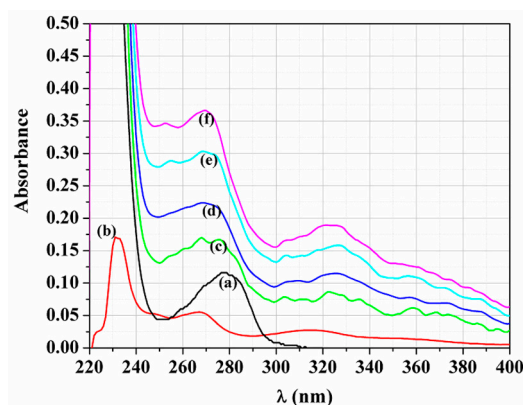


**Figure 7.** UV spectra of (a) 1.5  $\mu\text{M}$  BSA; (b) 20  $\mu\text{M}$  compound 3; (c) compound 3 (3.0  $\mu\text{M}$ ) + BSA (1.5  $\mu\text{M}$ ); (d) compound 3 (6.0  $\mu\text{M}$ ) + BSA (1.5  $\mu\text{M}$ ); (e) compound 3 (9.0  $\mu\text{M}$ ) + BSA (1.5  $\mu\text{M}$ ); (f) compound 3 (12  $\mu\text{M}$ ) + BSA (1.5  $\mu\text{M}$ ).

### 3.7. Effect of Compound 3 on BSA Conformation

#### 3.7.1. Synchronous Fluorescence

The synchronous fluorescence spectra of BSA indicate that the fluorescence of tyrosine (Tyr) and tryptophan (Trp) residues of BSA at wavelength intervals of  $\Delta\lambda$  is 15 and 60 nm, respectively [50,51]. It can be seen from Figure 8 that the intensity of the emission spectra of Tyr and Trp was diminished with no clear peak shift. When comparing the quenching effect of compound 3 on the fluorescence intensity of Tyr and Trp residues, it is clear that Trp quenching is more significant, which may refer to the fact that the binding site of compound 3 is nearer to the Trp residue.

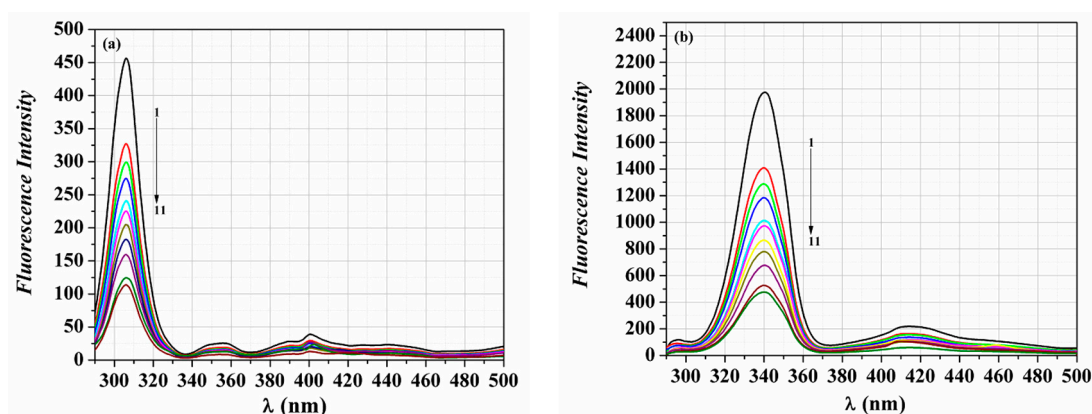


**Figure 8.** Spectra of the synchronous fluorescence of BSA (1.5  $\mu\text{M}$ ) with the addition of compound 3 (1–11) = (0–25  $\mu\text{M}$ ) at  $\Delta\lambda = 15$  nm (a)  $\Delta\lambda = 60$  nm (b).

#### 3.7.2. Three Dimensional Fluorescence Measurements

Measurements of the three-dimensional (3D) fluorescence were performed and the calculations of different characteristic 3D parameters are reported in Table 3. Figures 9 and 10 show that BSA

possesses different fluorescence peaks, where peak 1 ( $\lambda_{ex}$  224  $\rightarrow$   $\lambda_{em}$  336) is controversial as numerous previous studies have claimed that it originated from the  $n \rightarrow \pi^*$  transition of the polypeptide backbone of the serum albumin structure, correlating its intensity to the BSA or HAS (Human Albumin Serum) secondary structures [38,52]. Conversely, in a latest multi-laboratory investigation reported by Bortolotti et al. [53], it was established that this observed emission peak, following the excitation at 220–230 nm, aroused from Tyr and/or Trp. Therefore, this peak cannot provide any information on the backbone conformation of the protein. Peak 2 ( $\lambda_{ex}$  278  $\rightarrow$   $\lambda_{em}$  334) infers the spectral attributes of the Trp and Tyr residues [20]. With its binding to compound 3, the BSA fluorescence peaks were quenched, as evidenced from Figures 9b and 10b.

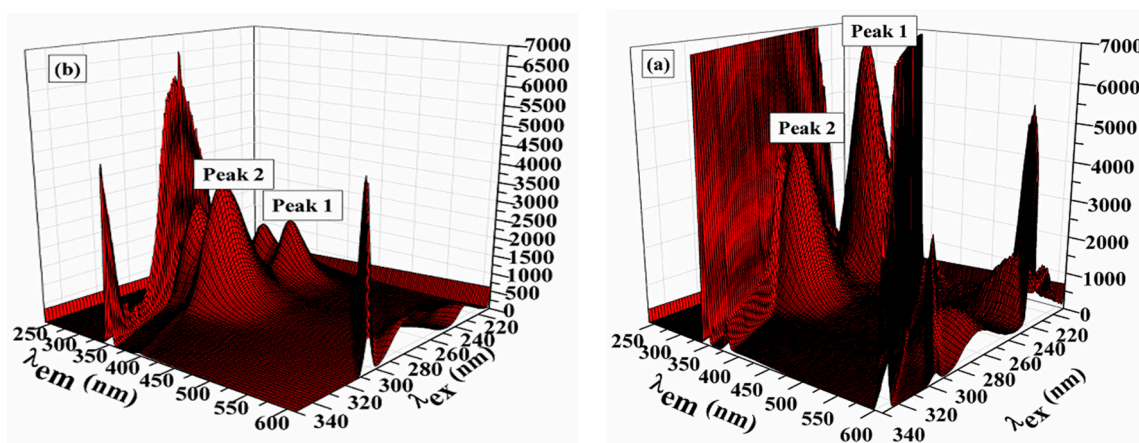


Figure 9. 3D spectra of BSA (1.5 μM) in (a) absence and (b) presence of compound 3 (12.0 μM).

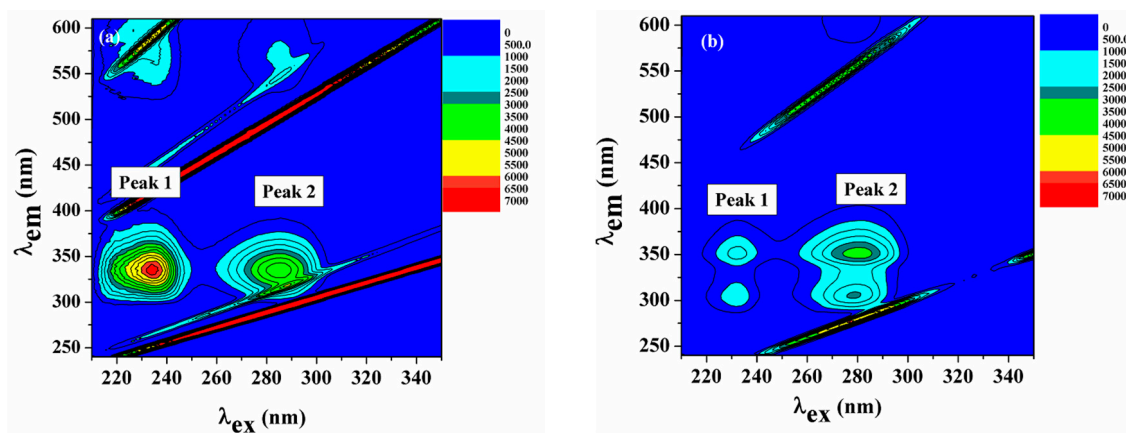


Figure 10. Contour plot of the fluorescence intensity spectra of BSA (a) compound 3-BSA system (b).

Table 3. Parameters of the 3D fluorescence for compound 3-BSA binding.

	BSA		Compound 3-BSA	
	1st Peak	2nd Peak	1st Peak	2nd Peak
Position of the peak ( $\lambda_{ex}/\lambda_{em}$ , nm/nm)	224/336	278/334	224/336	278/334
Relative intensity (IF)	9993.22	4258.31	2845.65	1290.87
Stokes shift $\lambda$ /nm	112	56	112	52

### 3.8. Site Markers Competitive Binding

Earlier reports have demonstrated that BSA, in similarity to HSA, has two main ligand-binding sites (I and II) located in subdomains IIA and IIIA, respectively [54–56]. Therefore, in order to comprehensively elaborate the BSA binding sites for the compound 3 interaction, the BSA binding to warfarin (WAR) and ibuprofen (IBP) was examined, as those two ligands were reported earlier as markers for the subdomains IIA and IIIA, respectively [54,55]. Fluorescence measurements were carried out for solutions of BSA and site markers (1:1 ratio) incrementally titrated with compound 3. Subsequent plots of Stern–Volmer (Equation (3)) and the double-log (Equation (6)) relations were graphed as shown in Figure 11. Constant values of  $K_{SV}$  and  $K$  were estimated from the plots and are listed in Table 4. The observed results unambiguously demonstrate that compound 3–BSA binding in the presence of WAR led to a remarkable decrease in  $K_{SV}$  and  $K$  values, in contrast to compound 3–BSA only, whilst nearly maintaining equal values in the presence of IBP. Hence, a displacement interaction between compound 3 and WAR on the BSA binding site can be concluded, which shows that compound 3 binds to the BSA subdomain IIA.

**Table 4.** Binding constant of compound 3 with the co-solution of BSA and site markers.

Systems	$K_{SV} \times 10^5$ (L·mol <sup>-1</sup> )	$r^2$
BSA + compound 3	$1.10 \pm 0.05$	0.9876
BSA + compound 3 + IBP	$1.08 \pm 0.06$	0.9782
BSA + compound 3 + WAR	$0.91 \pm 0.05$	0.9823

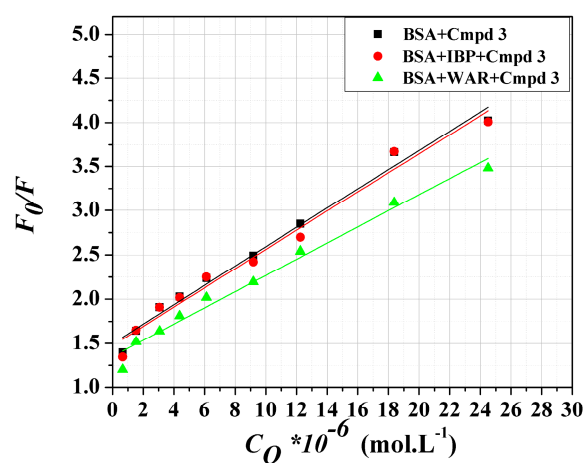


**Figure 11.** Stern–Volmer correlation derived from the BSA interaction with compound 3 at 298 K in the presence of WAR and IBP as the site markers.

### 3.9. Molecular Docking

Molecular docking as a simulation approach is a useful technique that links the protein and the ligand via various forms of interactions. It provides a validation tool to the experimental data obtained for the binding affinity and interaction modes of the ligand in the protein binding site. The complementary applications of molecular docking have been employed to improve the understanding of the interaction of compound 3 and BSA. The observed docking results for the compound 3–BSA system show that compound 3 binds to site I (subdomain IIA) in the BSA structure (Figure 12), which is complimented with the results acquired from site marker displacement studies. The scoring of the best conformation of compound 3 when bound to BSA demonstrated the lowest binding energy conformer that binds to BSA with a free energy of  $-25.94$  kJ·mol<sup>-1</sup> and RMSD of 1.146. This compound 3 conformer is situated within the active site residues Glu152, Tyr156, Ser191, Arg194, Leu197, Arg198, Ser201, Ala209, Trp213, Arg217, His287, Ala290, Glu291, Val342, Ser343,

Leu346, Asp450, Leu454, Leu480 and Val481 (Figure 12). Further, compound 3 was shown to form three hydrogen bonds with BSA through residues ASP450, Arg194 and Arg198, as summarized in Table 5. The observed docking results are consistent with the previously mentioned experimental data, confirming the tight binding between compound 3 and BSA via hydrogen bonding and electrostatic interactions. Furthermore, this finding provides a good structural basis to explain the efficient fluorescence quenching of BSA emission in the presence of compound 3. Binding to serum albumins controls the free, active concentration of a drug, provides a reservoir for a long duration of action, and ultimately affects drug absorption, metabolism, distribution, and excretion. Hence, the obtained docking results have further mapped the binding location and strength of compound 3 to the BSA.

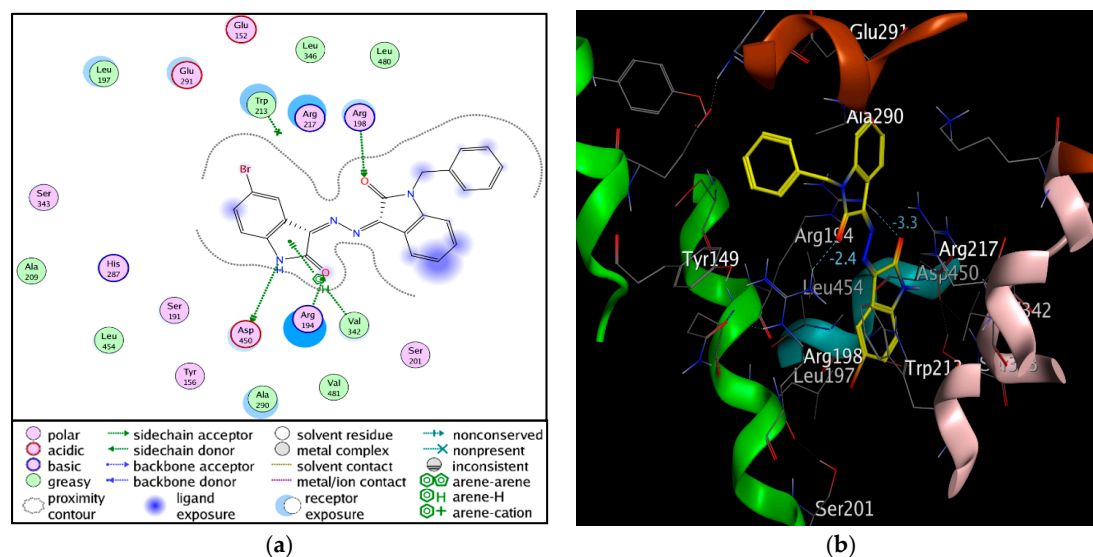


**Figure 12.** (a) A schematic demonstration, and (b) A cartoon illustration of the amino acids included in compound 3-BSA binding within the BSA site I binding pocket.

**Table 5.** Summary of the docking data obtained for compound 3 and BSA.

Compound 3	BSA Residues	Interaction Type	Distance (Å)
N 27	ASP450	H-donor	3.10
O 1	ARG198	H-acceptor	2.70
O 30	ARG194	H-acceptor	2.96
5-ring	VAL342	pi-H	4.50

#### 4. Conclusions

The current study focused on the synthesis of a new highly active anti-proliferative non-symmetric bis-isatin derivative. A subsequent comprehensive investigation of the BSA binding features of compound 3 using a fluorescence-quenching procedure was performed. Compound 3 was able to quench the fluorescence of BSA statically through the formation of a complex. Constants estimated from Stern–Volmer, Linweaver–Burk, and double log relations for the fluorescence emission data of the compound 3-BSA system were in the order of  $10^5 \text{ L} \cdot \text{mol}^{-1}$ , thus revealing the strong protein binding of compound 3. The computed thermodynamic parameters and molecular docking studies infer a spontaneous interaction that may involve both hydrogen bonding and electrostatic forces. The clinical consequences of drug-albumin interactions can be better understood with the aid of such studies, for example, dosage schedules can be empirically devised for highly albumin-bound drugs which are based on normal concentrations and the drug-binding behavior of albumin. Ultimately, due to the diversified functions of the serum albumins, more specifically their molecule transportation

role, the present study can play a crucial role in evaluating the pharmacological characteristics of compound **3** during further in vivo studies.

**Acknowledgments:** This project was funded by the National Plan for Science, Technology and Innovation (MAARIFAH), King Abdulaziz City for Science and Technology, Kingdom of Saudi Arabia, Award Number 11-MED1924-02.

**Author Contributions:** Ali Saber Abdelhameed, Hatem A. Abdel-Aziz and Mohamed I. Attia conceived and designed the experiments; Ahmed H. Bakheit, Mostafa S. Mohamed and Wagdy M. Eldehna performed the experiments; Ali Saber Abdelhameed analyzed the data; Ali Saber Abdelhameed, Hatem A. Abdel-Aziz and Mohamed I. Attia. contributed reagents/materials/analysis tools; Ali Saber Abdelhameed and Mohamed I. Attia wrote the paper.

**Conflicts of Interest:** The authors have declared no conflict of interest.

## References

1. Avendaño, C.; Menendez, J.C. *Medicinal Chemistry of Anticancer Drugs*; Elsevier: Amsterdam, The Netherlands, 2015.
2. Glover, V.; Halket, J.M.; Watkins, P.J.; Clow, A.; Goodwin, B.L.; Sandler, M. Isatin: Identity with the purified endogenous monoamine oxidase inhibitor tribulin. *J. Neurochem.* **1988**, *51*, 656–659. [[CrossRef](#)] [[PubMed](#)]
3. Sharma, V.M.; Prasanna, P.; Seshu, K.V.; Renuka, B.; Rao, C.V.; Kumar, G.S.; Narasimhulu, C.P.; Babu, P.A.; Puranik, R.C.; Subramanyam, D.; et al. Novel indolo[2,1-b]quinazoline analogues as cytostatic agents: Synthesis, biological evaluation and structure-activity relationship. *Bioorg. Med. Chem. Lett.* **2002**, *12*, 2303–2307. [[CrossRef](#)]
4. Gursoy, A.; Karali, N. Synthesis and primary cytotoxicity evaluation of 3-[[[(3-phenyl-4(3H)-quinazolinone-2-yl)mercaptoacetyl]hydrazono]-1H-2-indolinones. *Eur. J. Med. Chem.* **2003**, *38*, 633–643. [[CrossRef](#)]
5. Pandeya, S.N.; Smitha, S.; Jyoti, M.; Sridhar, S.K. Biological activities of isatin and its derivatives. *Acta Pharm.* **2005**, *55*, 27–46. [[PubMed](#)]
6. Moon, M.J.; Lee, S.K.; Lee, J.W.; Song, W.K.; Kim, S.W.; Kim, J.I.; Cho, C.; Choi, S.J.; Kim, Y.C. Synthesis and structure-activity relationships of novel indirubin derivatives as potent anti-proliferative agents with CDK2 inhibitory activities. *Bioorg. Med. Chem.* **2006**, *14*, 237–246. [[CrossRef](#)] [[PubMed](#)]
7. Cerchiaro, G.; Ferreira, A.M.D.C. Oxindoles and copper complexes with oxindole-derivatives as potential pharmacological agents. *J. Braz. Chem. Soc.* **2006**, *17*, 1473–1485. [[CrossRef](#)]
8. Eldehna, W.M.; Almahli, H.; Al-Ansary, G.H.; Ghabbour, H.A.; Aly, M.H.; Ismael, O.E.; Al-Dhfyhan, A.; Abdel-Aziz, H.A. Synthesis and in vitro anti-proliferative activity of some novel isatins conjugated with quinazoline/phthalazine hydrazines against triple-negative breast cancer MDA-MB-231 cells as apoptosis-inducing agents. *J. Enzyme Inhib. Med. Chem.* **2017**, *32*, 600–613. [[CrossRef](#)] [[PubMed](#)]
9. Sun, L.; Liang, C.; Shirazian, S.; Zhou, Y.; Miller, T.; Cui, J.; Fukuda, J.Y.; Chu, J.Y.; Nematalla, A.; Wang, X.; et al. Discovery of 5-[5-fluoro-2-oxo-1,2-dihydroindol-(3Z)-ylidenemethyl]-2,4-dimethyl-1H-pyrrole-3-carboxylic acid (2-diethylaminoethyl) amide, a novel tyrosine kinase inhibitor targeting vascular endothelial and platelet-derived growth factor receptor tyrosine kinase. *J. Med. Chem.* **2003**, *46*, 1116–1119. [[PubMed](#)]
10. Prenen, H.; Cools, J.; Mentens, N.; Folens, C.; Sciot, R.; Schoffski, P.; Van Oosterom, A.; Marynen, P.; Debiec-Rychter, M. Efficacy of the kinase inhibitor SU11248 against gastrointestinal stromal tumor mutants refractory to imatinib mesylate. *Clin. Cancer Res.* **2006**, *12*, 2622–2627. [[CrossRef](#)] [[PubMed](#)]
11. Motzer, R.J.; Michaelson, M.D.; Redman, B.G.; Hudes, G.R.; Wilding, G.; Figlin, R.A.; Ginsberg, M.S.; Kim, S.T.; Baum, C.M.; DePrimo, S.E.; et al. Activity of SU11248, a multitargeted inhibitor of vascular endothelial growth factor receptor and platelet-derived growth factor receptor, in patients with metastatic renal cell carcinoma. *J. Clin. Oncol.* **2006**, *24*, 16–24. [[CrossRef](#)] [[PubMed](#)]
12. Krug, M.; Hilgeroth, A. Recent advances in the development of multi-kinase inhibitors. *Mini Rev. Med. Chem.* **2008**, *8*, 1312–1327. [[CrossRef](#)] [[PubMed](#)]
13. Liang, C.; Xia, J.; Lei, D.; Li, X.; Yao, Q.; Gao, J. Synthesis, in vitro and in vivo antitumor activity of symmetrical bis-Schiff base derivatives of isatin. *Eur. J. Med. Chem.* **2014**, *74*, 742–750. [[CrossRef](#)] [[PubMed](#)]
14. Kragh-Hansen, U. Molecular aspects of ligand binding to serum albumin. *Pharmacol. Rev.* **1981**, *33*, 17–53. [[PubMed](#)]
15. He, X.M.; Carter, D.C. Atomic structure and chemistry of human serum albumin. *Nature* **1992**, *358*, 209–215. [[CrossRef](#)] [[PubMed](#)]

16. Bhattacharya, A.A.; Grune, T.; Curry, S. Crystallographic analysis reveals modes of binding of medium and long chain fatty acids to human serum albumin. *J. Mol. Biol.* **2000**, *303*, 721–732. [[CrossRef](#)] [[PubMed](#)]
17. Sattar, Z.; Iranfar, H.; Asoodeh, A.; Saberi, M.R.; Mazhari, M.; Chamani, J. Interaction between holo transferrin and HSA–PPIX complex in the presence of lomefloxacin: An evaluation of PPIX aggregation in protein–protein interactions. *Spectrochim. Acta Part A* **2012**, *97*, 1089–1100. [[CrossRef](#)] [[PubMed](#)]
18. Tian, J.; Liu, J.; Hu, Z.; Chen, X. Interaction of wogonin with bovine serum albumin. *Bioorg. Med. Chem.* **2005**, *13*, 4124–4129. [[CrossRef](#)] [[PubMed](#)]
19. Abdelhameed, A.S. Insight into the Interaction between the HIV-1 Integrase inhibitor Elvitegravir and bovine serum albumin: A Spectroscopic study. *J. Spectrosc.* **2015**. [[CrossRef](#)]
20. Sułkowska, A. Interaction of drugs with bovine and human serum albumin. *J. Mol. Struct.* **2002**, *614*, 227–232. [[CrossRef](#)]
21. Zhou, N.; Liang, Y.Z.; Wang, P. 18 $\beta$ -Glycyrrhetic acid interaction with bovine serum albumin. *J. Photochem. Photobiol. A* **2007**, *185*, 271–276. [[CrossRef](#)]
22. Wang, Y.Q.; Zhang, H.M.; Zhang, G.C.; Tao, W.H.; Fei, Z.H.; Liu, Z.T. Spectroscopic studies on the interaction between silicotungstic acid and bovine serum albumin. *J. Pharm. Biomed. Anal.* **2007**, *43*, 1869–1875. [[CrossRef](#)] [[PubMed](#)]
23. Wang, Y.P.; Wei, Y.L.; Dong, C. Study on the interaction of 3,3-bis(4-hydroxy-1-naphthyl)-phthalide with bovine serum albumin by fluorescence spectroscopy. *J. Photochem. Photobiol. A* **2006**, *177*, 6–11. [[CrossRef](#)]
24. Bolel, P.; Mahapatra, N.; Halder, M. Optical spectroscopic exploration of binding of cochineal red A with two homologous serum albumins. *J. Agric. Food Chem.* **2012**, *60*, 3727–3734. [[CrossRef](#)] [[PubMed](#)]
25. Carter, D.C.; Ho, J.X. Structure of serum albumin. *Adv. Protein Chem.* **1994**, *45*, 153–203. [[PubMed](#)]
26. Gong, A.; Zhu, X.; Hu, Y.; Yu, S. A fluorescence spectroscopic study of the interaction between epristeride and bovin serum albumine and its analytical application. *Talanta* **2007**, *73*, 668–673. [[CrossRef](#)] [[PubMed](#)]
27. Zhou, B.; Qi, Z.D.; Xiao, Q.; Dong, J.X.; Zhang, Y.Z.; Liu, Y. Interaction of loratadine with serum albumins studied by fluorescence quenching method. *J. Biochem. Biophys. Methods* **2007**, *70*, 743–747. [[CrossRef](#)] [[PubMed](#)]
28. Eldehna, W.M.; Altoukhy, A.; Mahrous, H.; Abdel-Aziz, H.A. Design, synthesis and QSAR study of certain isatin-pyridine hybrids as potential anti-proliferative agents. *Eur. J. Med. Chem.* **2015**, *90*, 684–694. [[CrossRef](#)] [[PubMed](#)]
29. Schmidt, M.S.; Reverdito, A.M.; Kremenchuzky, L.; Perillo, I.A.; Blanco, M.M. Simple and efficient microwave assisted N-alkylation of isatin. *Molecules* **2008**, *13*, 831–840. [[CrossRef](#)] [[PubMed](#)]
30. Keeton, A.B.; Piazza, G.A.; University of South Alabama, Alabama, AL, USA. Unpublished work. 2017.
31. Dufour, C.; Dangles, O. Flavonoid–serum albumin complexation: Determination of binding constants and binding sites by fluorescence spectroscopy. *Biochim. Biophys. Acta Gen. Subj.* **2005**, *1721*, 164–173. [[CrossRef](#)] [[PubMed](#)]
32. Lakowicz, J.R. *Principles of Fluorescence Spectroscopy*; Springer Science & Business Media, LLC: New York, NY, USA, 2007.
33. Bujacz, A.; Zielinski, K.; Sekula, B. Structural studies of bovine, equine, and leporine serum albumin complexes with naproxen. *Proteins Struct. Funct. Bioinf.* **2014**, *82*, 2199–2208. [[CrossRef](#)] [[PubMed](#)]
34. Pasban Ziyarat, F.; Asoodeh, A.; Sharif Barfeh, Z.; Pirouzi, M.; Chamani, J. Probing the interaction of lysozyme with ciprofloxacin in the presence of different-sized Ag nano-particles by multispectroscopic techniques and isothermal titration calorimetry. *J. Biomol. Struct. Dyn.* **2014**, *32*, 613–629. [[CrossRef](#)] [[PubMed](#)]
35. Bourassa, P.; Bariyanga, J.; Tajmir-Riahi, H.A. Binding Sites of Resveratrol, Genistein, and Curcumin with Milk  $\alpha$ - and  $\beta$ -Caseins. *J. Phys. Chem. B* **2013**, *117*, 1287–1295. [[CrossRef](#)] [[PubMed](#)]
36. Hu, Y.; Da, L. Insights into the selective binding and toxic mechanism of microcystin to catalase. *Spectrochim. Acta Part A* **2014**, *121*, 230–237. [[CrossRef](#)] [[PubMed](#)]
37. Lakowicz, J.R. *Principle of Fluorescence Spectroscopy*, 2nd ed.; Plemum Press: New York, NY, USA, 1999.
38. Zhang, W.; Wang, F.; Xiong, X.; Ge, Y.; Liu, Y. Spectroscopic and molecular docking studies on the interaction of dimetridazole with human serum albumin. *J. Chil. Chem. Soc.* **2013**, *58*, 1717–1721. [[CrossRef](#)]
39. Shcharbin, D.; Klajnert, B.; Mazhul, V.; Bryszewska, M. Dendrimer Interactions with Hydrophobic Fluorescent Probes and Human Serum Albumin. *J. Fluoresc.* **2005**, *15*, 21–28. [[CrossRef](#)] [[PubMed](#)]
40. Stern, O.; Volmer, M. The extinction period of fluorescence. *Phys. Z.* **1919**, *20*, 183–188.

41. Lineweaver, H.; Burk, D. The determination of enzyme dissociation constants. *J. Am. Chem. Soc.* **1934**, *56*, 658–666. [[CrossRef](#)]
42. Lakowicz, J.R.; Weber, G. Quenching of fluorescence by oxygen. Probe for structural fluctuations in macromolecules. *Biochemistry* **1973**, *12*, 4161–4170. [[CrossRef](#)] [[PubMed](#)]
43. Huang, Y.; Zhang, Z.; Zhang, D.; Lv, J. Flow-injection analysis chemiluminescence detection combined with microdialysis sampling for studying protein binding of drug. *Talanta* **2001**, *53*, 835–841. [[CrossRef](#)]
44. Ware, W.R. Oxygen quenching of fluorescence in solution: An experimental study of the diffusion process. *J. Phys. Chem.* **1962**, *66*, 455–458. [[CrossRef](#)]
45. Chen, G.Z.; Huang, X.Z.; Xu, J.G. *Spectrofluorimetric Analytical Method*, 2nd ed.; Science Press: Beijing, China, 1990.
46. Liu, J.; Tian, J.N.; Zhang, J.; Hu, Z.; Chen, X. Interaction of magnolol with bovine serum albumin: A fluorescence-quenching study. *Anal. Bioanal. Chem.* **2003**, *376*, 864–867. [[PubMed](#)]
47. Forster, T.; Sinanoglu, O. *Modern Quantum Chemistry*; Academic Press: New York, NY, USA, 1996; p. 93.
48. Ross, P.D.; Subramanian, S. Thermodynamics of protein association reactions: Forces contributing to stability. *Biochemistry* **1981**, *20*, 3096–3102. [[CrossRef](#)] [[PubMed](#)]
49. Abdelhameed, A.S.; Alanazi, A.M.; Bakheit, A.H.; Darwish, H.W.; Ghabbour, H.A.; Darwish, I.A. Fluorescence spectroscopic and molecular docking studies of the binding interaction between the new anaplastic lymphoma kinase inhibitor crizotinib and bovine serum albumin. *Spectrochim. Acta Part A* **2017**, *171*, 174–182. [[CrossRef](#)] [[PubMed](#)]
50. Yan, H.; Zhao, S.; Yang, J.; Zhu, X.; Dai, G.; Liang, H.; Pan, F.; Weng, L. Interaction between Levamisole hydrochloride and bovine serum albumin and the influence of alcohol: Spectra. *J. Solut. Chem.* **2009**, *38*, 1183–1192. [[CrossRef](#)]
51. Zhang, H.X.; Huang, X.; Mei, P.; Gao, S. Interaction between Glyoxal-bis-(2-hydroxyanil) and bovine serum albumin in solution. *J. Solut. Chem.* **2008**, *37*, 631–640. [[CrossRef](#)]
52. Samanta, A.; Paul, B.K.; Guchhait, N. Spectroscopic probe analysis for exploring probe–protein interaction: A mapping of native, unfolding and refolding of protein bovine serum albumin by extrinsic fluorescence probe. *Biophys. Chem.* **2011**, *156*, 128–139. [[CrossRef](#)] [[PubMed](#)]
53. Bortolotti, A.; Wong, Y.H.; Korsholm, S.S.; Bahring, N.H.B.; Bobone, S.; Tayyab, S.; Van De Weert, M.; Stella, L. On the purported “backbone fluorescence” in protein three-dimensional fluorescence spectra. *RSC Adv.* **2016**, *6*, 112870–112876. [[CrossRef](#)]
54. Ghuman, J.; Zunszain, P.A.; Petitpas, I.; Bhattacharya, A.A.; Otagiri, M.; Curry, S. Structural basis of the drug-binding specificity of human serum albumin. *J. Mol. Biol.* **2005**, *353*, 38–52. [[CrossRef](#)] [[PubMed](#)]
55. Chaturvedi, S.K.; Ahmad, E.; Khan, J.M.; Alam, P.; Ishtikhar, M.; Khan, R.H. Elucidating the interaction of limonene with bovine serum albumin: A multi-technique approach. *Mol. Biosyst.* **2015**, *11*, 307–316. [[CrossRef](#)] [[PubMed](#)]
56. Sudlow, G.; Birkett, D.; Wade, D. Further characterization of specific drug binding sites on human serum albumin. *Mol. Pharmacol.* **1976**, *12*, 1052–1061. [[PubMed](#)]

